PERGAMON

Deep-Sea Research II 49 (2002) 1011–1027

DEEP-SEA RESEARCH
PART II

www.elsevier.com/locate/dsr2

Calcareous plankton stratigraphy around the Pliocene "Eltanin" asteroid impact area (SE Pacific): documentation and application for geological and paleoceanographic reconstruction

J.-A. Flores[a,*], F.J. Sierro[a], R. Gersonde[b]

[a] *Facultad de Ciencias, Universidad de Salamanca, E-37008 Salamanca, Spain*
[b] *Alfred Wegener Institute for Polar and Marine Research, D-27515 Bremerhaven, Germany*

Abstract

Conventional qualitative and semi quantitative analyses of calcareous nannofossils and planktic foraminifers from four cores (PS2704-1, PS2708-1, PS2709-1, E13-4) documenting the area of the Eltanin impact into the Bellingshausen Sea were done to (a) identify sediment disturbances and reworking, (b) constrain the stratigraphic framework of the impact-related sediment sequences, and (c) evaluate probable environmental consequences of the impact. The calcareous microfossil stratigraphy from the autochthonous sediments above and below the impact-related sediments places the impact event into the late Pliocene at around 2.15 Ma, and indicates that sediments as old as middle Eocene were disturbed by the impact. The qualitative and quantitative determination of displaced calcareous microfossils allows the reconstruction of sediment disturbances, displacement, and resettlement related to the impact event. No signs for significant changes in the assemblages produced and sedimented after the impact could be observed, indicating that the impact had no major influence on regional or global climate conditions that can be detected in the geological record.

1. Introduction and objectives

Microfossil analysis of marine sediments related to extraterrestrial impacts is a common tool for biostratigraphic and paleoenvironmental reconstruction. Undoubtedly, the Cretaceous/Tertiary boundary impact is the most significant event in which planktic microfossil biostratigraphy and paleoecology have been used for general reconstruction (e.g., Sidgurdsson et al., 1997). The Eocene is another interval where impact-related structures or material (e.g., microtektites) have been studied, dated or interpreted using micropaleontological techniques (Keller, 1983, 1986; Keller et al., 1983, 1987; Aubry et al., 1990; Wei, 1995).

In the mid-1960s, the USNS "Eltanin" recovered several cores in the Bellingshausen Sea (Pacific sector of the Southern Ocean; Fig. 1). Studying the Eltanin cores, Kyte et al. (1981) discovered an Iridium anomaly, linked to the presence of extraterrestrial material input in the

*Corresponding author. Tel.: +34-923-294-497; fax: +34-923-294514.
E-mail address: flores@usal.es (J.-A. Flores).

0967-0645/02/$ - see front matter
PII: S0967-0645(01)00137-0

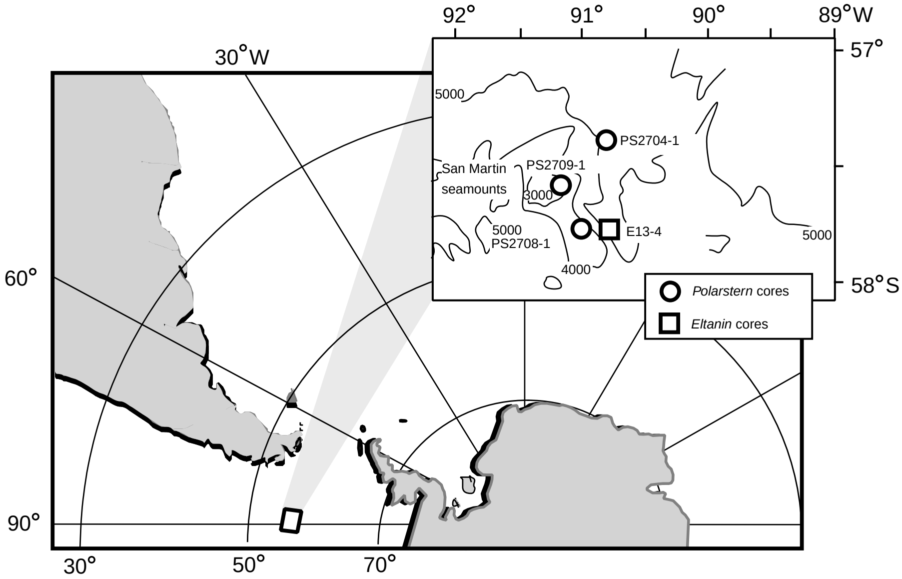

Fig. 1. Geographical location of cores used in this study.

sediments. Later on, Kyte and Brownlee (1985), Kyte and Smit (1986) and Margolis et al. (1990) identified ejecta particles and other evidence of an extraterrestrial body, interpreted as a basaltic achondrite (an anomalous mesosiderite), and named it the "Eltanin meteorite".

A more comprehensive exploration of the Eltanin impact area was accomplished in 1995 during expedition ANT-XII/4 of the R.V. "*Polarstern*". This survey combined bathymetric, seismic and marine-geological studies in the area of the San Martin Seamounts, where highest concentrations of impact debris have been encountered during the previous studies (Kyte et al., 1988). The obtained acoustic data and sediment samples allowed Gersonde et al. (1997) to reconstruct and reinterpret the impact scenario. These authors found evidence of erosion and re-deposition of sediments covering the time-span of the last 50 m.y. (Fig. 1). According to Gersonde et al. (1997), this sediment disturbance was produced by the impact of an asteroid, 1–4 km in diameter, in the deep ocean during the late Pliocene (ca. 2.15 Ma).

In this study we report results from calcareous nannofossil and planktic foraminifers analyses focusing on: (1) the age of the impact, using combined biostratigraphy schemes; (2) dating the undisturbed materials that underlie the disturbed sediments; (3) reworking and identification of the age and provenance in the mixed layers; and (4) paleoenvironmental characteristics of the calcareous plankton after the impact event.

2. Material and micropaleontological techniques

2.1. Study area and sediment cores

The studied region is located on the Pacific-Aluk portion of the Antarctic plate, in the Bellingshausen Sea (Fig. 1). In the abyssal portions of this area high-resolution seismic survey with Parasound echosounding has revealed an acoustically well-stratified sequence, underlain by a seismically transparent sediments with a thickness between 20 and 60 m, named the "Eltanin-Polarstern Transparent Zone" (EPTZ) and interpreted as

Table 1
Location and water-depth of the RV Polarstern and Eltanin cores

Core	Situation	Depth (m)
PS2709-1	57°46.8′S, 90°59.9′W	2707
PS2708-1	57°35.4′S, 91°13.2′W	3965
PS2704-1	57°23.4′S, 90°48.4′W	4961
E13-4	57°47.2′S, 90°47.6′W	4700

being impact-related (Gersonde et al., 1997). In the area of highest flux of meteoritic ejecta bathymetric mapping revealed a complex topographic high with minimum water depths of ca. 2500 m, named the San Martin Seamounts. The surrounding abyssal areas have depths around 5000 m. Here we present micropaleontological data from three sediment cores recovered during the ANT-XII/4 expedition. The cores form a depth profile from the top of the seamount (PS2709-1), to intermediate water depths at the seamount's slope (PS2708-1), to the abyssal basin, east of the seamount (PS2704-1) (Fig. 1; Table 1). From these cores Gersonde et al. (1997) defined five sedimentary units (SU I–V), which document the impact event as well as autochthonous sediments below and above the impact-related sequences. Additionally, Eltanin core E13-4, located close to the assumed impact site, was analyzed.

2.2. *Calcareous nannofossils*

Standard unprocessed smear slides were made for all samples. Calcareous nannofossils were examined using a light-polarized microscope at 1000 × magnification. Unless otherwise indicated, we followed the taxonomic concepts summarized in Perch-Nielsen (1985). For morphometric concepts concerning the *Gephyrocapsa* group, we followed the proposal of Raffi et al. (1993).

Regarding nannofossil preservation, etching and overgrowth are the most important features. In order to establish a ranking of preservation we followed previous code systems, such as that used by Gersonde et al. (1999), considering both effects, etching and overgrowth:

G = good (little or no evidence of dissolution and/or secondary overgrowth of calcite; diagnostic characters fully preserved)
M = moderate (dissolution and/or secondary overgrowth: partially altered primary morphological characteristics: nearly all specimens can be identified at species level).
P = poor (severe dissolution, fragmentation, and/or secondary overgrowth with primary features largely destroyed; many specimens cannot be identified at species level and/or generic level).

The abundance of calcareous nannofossils was estimated using the following criteria:

V (very abundant) = > 50 specimens per field of view.
A (abundant) = 10–50 specimens per field of view.
C (common) = 1–9 specimens per field of view.
F (few) = 1 specimen per 2–10 fields of view.
R (rare) = 1 specimen in more than 11 fields of view.

Data concerning calcareous nannofossil abundance from different samples are provided in Tables 2–4. Additionally, the proportion between autochthonous and reworked nannofossils was estimated by counting about 300 specimens.

2.3. *Planktic foraminifers*

Samples for planktic foraminifers analyses were washed over a 63-μm mesh sieve and dry sieved at 125 μm. The residues were split into suitable aliquots of about 350 specimens, which were counted afterwards. The fragmentation index represents the ratio between whole planktic foraminiferal shells and whole plus fragmented shells. The content of the coarse-grained fraction is the weight percentage of the residue larger than 125 μm relative to the weight of the dry bulk sample.

Table 2
Relative abundance of calcareous nannofossil species in SU IV and SU V in the studied cores. Nomenclature given in the text (Section 2.2)

Species	Martini zone (Perch-Nielsen, 1985)	PS2708-1	PS2708-1	PS2704-1	PS2709-1	E 13-4
Coccolithus pelagicus gr.	Wide range	F	F	F	F	F
Coccolithus miopelagicus	NN 1?-NN 8				F	
Calcidiscus leptoporus	NN2?-recent		F	R	R	
Cyclicargolithus floridanus	NP 20-NN 6		F	C	C	
Chiasmolithus spp. (rims)	—	A	C	C	C	C
Chiasmolithus expansus	NP 12?-NP 16	F		F	F	
Chiasmolithus solitus	NP 12-NP 16	R		F	F	
Chiasmolithus oamaruensis	NP 18-NP 22?		F	R	R	
Chiasmolithus sp. cf. *S. grandis*	NP 11?- NP 17			R	R	
Reticulofenestra hillae = *R. samodurovii*	NP 14-NP 22	C	R	C	C	
Reticulofenestra umbilicus	NP 16-NP 22	C	R	C	C	
Reticulofenestra sp. cf. *R. pseudoumbilicus*	NN 7?-NN 15				F	
Reticulofenestra oamaruensis	NP 2-NP 22			R	R	
Reticulofenestra daviesii	NP 16-NP 21	F		F	F	
Reticulofenestra bisecta	NP 15-NP 25?			F	F	
Istmolithus recurvus	NP 19-NP 21				R	
Cribrocentrum reticulatum	NP 16-NP 19	R		R	R	
Cyclicargolithus protoannulus	NP 14?-NP 20	C		C	C	
Coronocyclus nitescens	NP17?-NN4?		F	R	R	
Ericsonia formosa	NP 12-NP 21	R		R	R	R
Neococcolithes dubius	NP 13-NP 18	R		R	R	C
Discoaster deflandrei	NP 11-NN 11			R	R	
Discoaster sublodoensis	NP 13-NP 15					F
Discoaster lodoensis	NP 12-NP 14					R
Discoaster septemradiatus	NP 12-NP 14					R
Discoaster spp.	—					C
Sphenolithus moriformis	NP 12-NN 9	R	F	R	R	R
Sphenolithus sp. cf. *S. abies*	NN 10-NN 15			F	F	
Stratigraphic unit		SU V	SU IV	SU IV	SU IV	SU IV
Interpretation		Eocene NP16	Mixed	Mixed	Mixed	Mixed

3. Calcareous microfossil composition of sedimentary units

3.1. Autochthonous undisturbed basal sediments—sedimentary unit V

This sedimentary unit (SU V) is well documented in core PS2708-1 (1275–1450 cm) (Fig. 2). The abundance of calcareous nannofossils in this interval is very high, with a moderate degree of preservation. A 20-cm interval analysis of this interval revealed a uniform nannofossil assemblage (Table 2). The presence of common *Reticulofenestra umbilicus*, whose first occurrence (FO) is situated in the standard Martini (1971) Zone NP 16, as well as the absence of other frequent species in the overlying "reworked" sediments, such as *Reticulofenestra bisecta* (FO in NP 17 Zone), allow us to assign a middle Eocene age (NP 16), about 41–43 Ma (Berggren et al., 1995) to these sediments. This suggests that the geomagnetic polarity sequence obtained from this interval represents an interval ranging from the top of Chron C20n to the base of Chron C18n.

The planktic foraminifers of unit SU V were only analyzed in core PS2708-1. All planktic foraminifers in this unit are of middle Eocene age, corresponding to the biozone of *Acarinina*

Table 3
Relative abundance of calcareous nannofossil species in SU I in core PS2709-1. Nomenclature given in the text (Section 2.2)

Depth (cm)	Abundance	Preservation	Small *Gephyrocapsa*	*P. lacunosa*	Medium *Gephyrocapsa*	*R. asanoi*	*C. pelagicus*	*C. leptoporus*	*H. carteri*	*Syracosphaera* spp.	Large *Gephyrocapsa*	Sedimentary unit
700	C	M	C	F		R	F	R	R			
710	A	G	V	F	R		C	F	R			
720	A	G	A	F	R	R	R	C				
725	A	G	V	C			R	F	F			
730	A	G	V	F	R	F		C				
740	A	G	V	F		F	R	C	F			
750	F	M	F	F	R	R	F	F				
755	F	M		R		R		F				
760	C	M	R	F	R	R	C	F				
770	A	G	A	F	F	F	F	R	R			
780	A	M	F	F		F	C	C				
820	A	M	F	R		F	A	R				
850	A	M	F	F		F	A	R				
860	A	M	R	R		R	A	C				
870	A	M	C	F		R	A	C				
890	A	M	R	R		R	A	F				
920	C	M	F	R		F	C	F				
930	A	G	V	F		C	A	C		F		
950	A	G	V	F		F	C	F	F			
960	A	G	V	R		R	A	F				
965	A	G	V	C		F	A	C		F		
970	C	M	R	F		C		C	R			
1000	C	M	R	C		F	F	F				
1040	C	M		C		R	R	F	R			
1050	C	M	R	C		F	F	C				
1060	C	M		C		R	F	C			R	
1065	C	M		C			C	R			R	
1070	C	M		C		R	C	F				
1080	C	M		F			C	R				
1090	F	M		F	?		F	R			R	
1095	F	M		F	R			F			C	
1100	F	M	R	F	R		F	F	F		F	
1105	F	M		F			R	F	F			SU I
1110	F	M		A	F		R	F			C	
1115	C	M		C	C		C	C			C	
1120	C	M		F	F		F	R			C	
1130	C	M	R	F	F			F	R		C	
1140	C	M		F	F		F	F			C	
1200	C	M	R	F	R		F	R			C	
1230	C	M	R	F	F		F	F			F	

Table 3 (*continued*)

Depth (cm)	Abundance	Preservation	Small *Gephyrocapsa*	*P. lacunosa*	Medium *Gephyrocapsa*	*R. asanoi*	*C. pelagicus*	*C. leptoporus*	*H. carteri*	*Syracosphaera* spp.	Large *Gephyrocapsa*	Sedimentary unit
1250	A	G	A	F	A		R	F	F		A	
1260	A	G	F	R	F		F	F	R		C	
1270	C	G		C	C		F	R			F	
1275	A	G		C	A		C	F			F	
1280	C	M	R	R	F		C	R				
1290	C	M	R	R	F		C	F				
1300	C	M	F	F	F		F	R				
1310	C	M	F	F	F		A	R				
1315	C	M	F	R	F		A	R	R			
1320	F	M	F	F			F	R				
1340	F	M	F	F			F	R				
1400	C	M		F			F	F				
1500	A	M		F			A	C				
1540	A	M	F	F			A	D		R		
1550	A	M		R			A	F		R		
1560	A	M		R			A	A		F		
1570	C	M		F			C	A				
1600	C	M		F			C	R		cf.		
1620	C	M		F				F				
1640	C	M		F			C	C				
1650	C	M		F			F					
1660	C	M		F			F	F				
1668	C	M		F			F	F				SU II
				Reworked dominant (Eocene–Miocene)								

Table 4
Relative abundance of calcareous nannofossil species in SU I in core PS2708-1. Nomenclature given in the text (Section 2.2)

Depth (cm)	Abundance	Preservation	Small *Gephyrocapsa*	*G. oceanica*	*G. caribbeanica*	*P. lacunosa*	Medium *Gephyrocapsa*	*R. asanoi*	*C. pelagicus*	*C. leptoporus*	*H. carteri*	Large *Gephyrocapsa*	Sedimentary unit
349	F	P	R			F			F	F			
363	F	P			R	F		F	F	R			
370	F	M	R	R?		F		F	F	R			
380	F	M	F			F		F	R	R			
400	C	M	R			R		F	C	F			
435	C	M	R			F	R	F	F	F			
463	C	M	R			R		R	C	R			
498	F	M				F		F	F	R	R		
530	C	M	R			F		R	A	F			
560	F	P				C		F	C	R			
600	F	M	R			F		F	F	R			SU I
630	F	M				R			F	R			
656	F	P				F			C	F			
690	F	P				F			R	F		R	
711	F	M				F			F	F		F	
740	C	M					R		F	F		F	
754	C	M							F	F		F	
781	F	M							F	R		F	
810	C	M				F	R		F	F		F	
820	F	M				F			R	R			
840	F	M	R			R	R		F	F			
854	F	M				F			C	F			
880	C	P				F			F	F			
897	C	M	Reworked dominant (Eocene–Miocene)										SU II

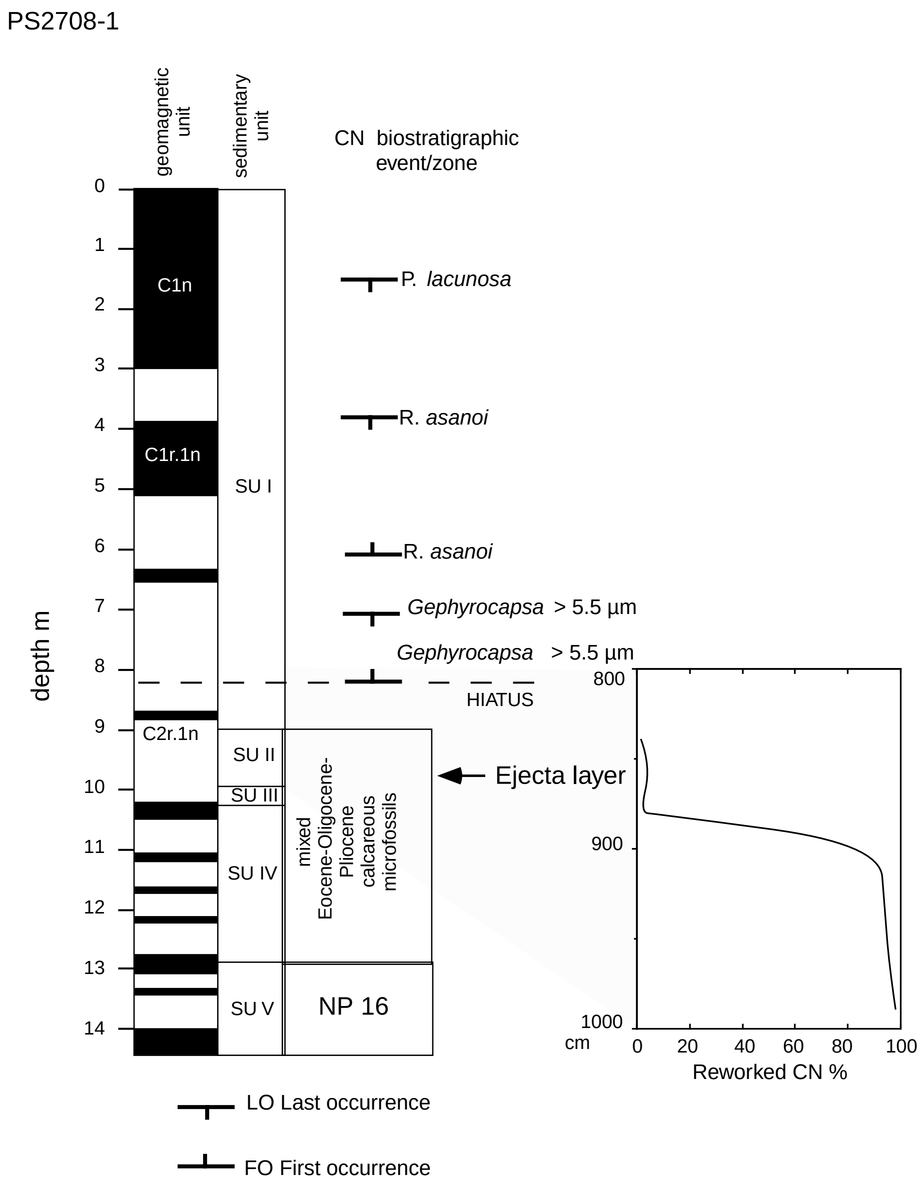

Fig. 2. Calcareous nannofossil biostratigraphic events and correlation with the geomagnetic signal and relative abundance of reworked calcareous nannofossil and planktic foraminifers in core PS2408-1. Geomagnetic polarity record and its stratigraphic interpretation as well as assignment of sedimentary units (SU) is according to Gersonde et al. (1997) CN = Calcareous nannofossils. Details of calcareous nannofossil composition given in Tables 2 and 4.

collactea of Berggren (1992). *Subbotina angiporoides, Globigerinatheca index, Acarinina primitiva*, and *Chiloguembelina cubensis* are the most frequent species. At the boundary between SU V and SU IV, planktic foraminifers are predominantly Eocene in age, but a few specimens of *Globorotalia puncticulata*, a typical Pliocene species, also have been encountered (Fig. 3).

In core PS2704-1, sediments attributed to SU V are barren of calcareous plankton due to its

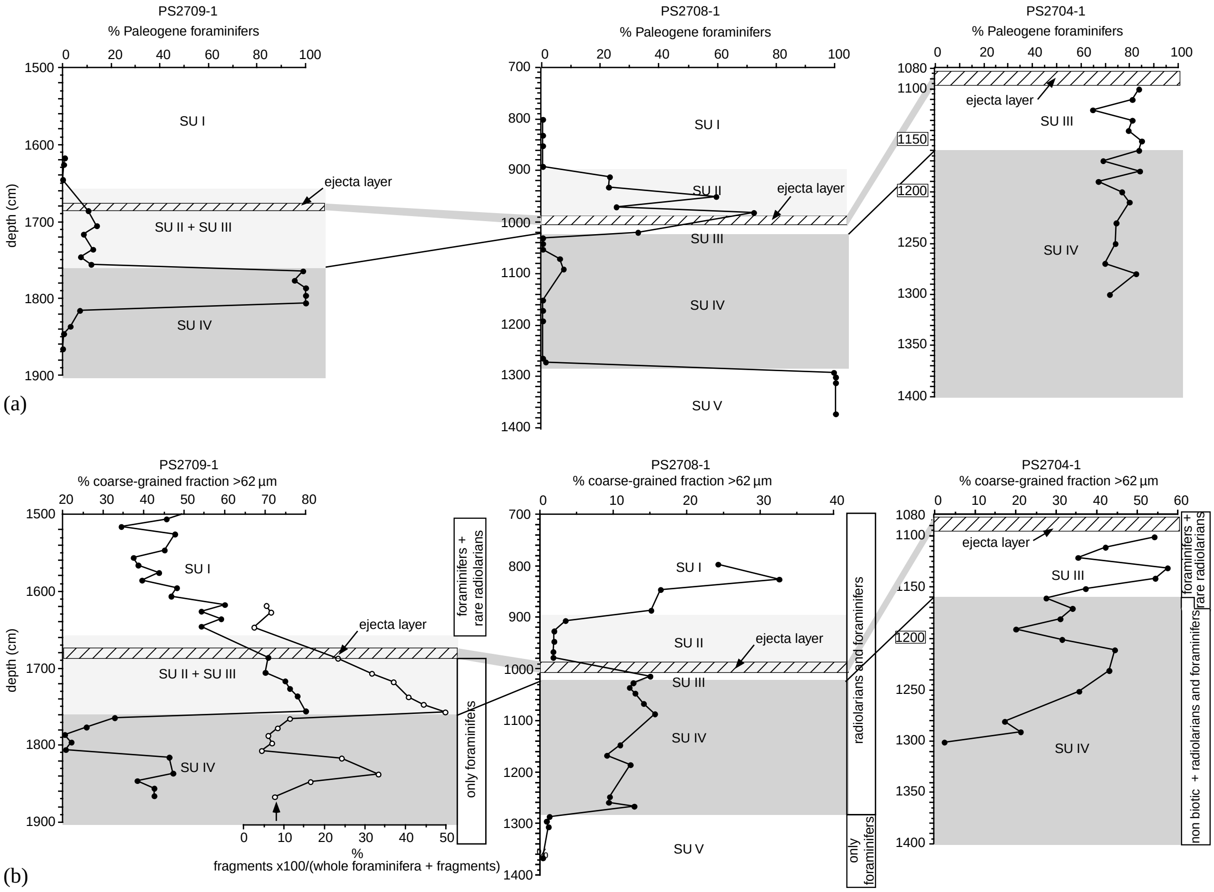

Fig. 3. (a) Downhole variation in percent of the Paleogene planktic foraminifers (number of Paleogene foraminifers × 100/total number of planktic foraminifers) in cores PS2709-1, PS2708-1, and PS2704-1. (b) Percentage of the coarse-grained fraction (weight of the residue > 62 μm × 100/weight of the bulk sample) in cores PS2709-1, PS2708-1, and PS2704-1. The fragmentation index of planktic foraminifers for core PS2709-1 is also shown. Vertical rectangles indicate the main biotic and non-biotic (e.g. manganese micronodules, lithogenic fragments) components of the coarse-grained fraction in each interval. Note the differences in depth scales. SU = sedimentary unit.

original position beneath the carbonate compensation depth (CCD) (see Table 1).

3.2. Impact-related deposits—sedimentary units IV, III, and II

3.2.1. Sedimentary unit IV

This unit (SU IV) composed by an allochthonous, chaotic mixture of sedimentary clasts with different ages and lithologies was identified in all studied cores, PS2708-1, PS2709-1 and PS2704-1. The species composition and stratigraphic range of the calcareous microfossils encountered in different clasts and samples from the associated sediment matrix are mixed, revealing no down-core sequence or pattern. Clasts in which calcareous nannofossils are absent alternate with others containing taxa labeled in Table 2, and include a mixture of Eocene–Oligocene species. In these cores, the matrix between the clasts contains disconnected shields of *Coccolithus pelagicus* and *Calcidiscus leptoporus* at various abundances ranging from rare to few as well as few *Reticulofenestra* sp. cf. *R. pseudoumbilicus*. Additional species identified also in the clasts, indicate a mixture of Paleogene and Neogene calcareous nannofossils. Samples taken from the lower portion of SU IV in core PS2704-1 are devoid of calcareous microfossils (Fig. 4).

Regarding planktic foraminifers, two intervals were distinguished in core PS2709-1: in the lower part (between the base and 1816 cm core depth), the faunas are predominantly of Pliocene age (Fig. 3). The most abundant species is *G. puncticulata*, and there are only very rare occurrences of species with an age-range extending from the middle Eocene to the lower Oligocene. Above this interval (between 1806 and 1764 cm core depth), the foraminifers are predominantly Paleogene in age. The encountered assemblages are dominated by *S. angiporoides* in the >125-μm fraction, and by *C. cubensis* in the >62-μm fraction. These two species are characteristic of the middle Eocene, late Eocene and early Oligocene in the Kerguelen Plateau area (Berggren, 1992). Both species were extremely abundant during the late Eocene. Pliocene assemblages were seen in samples at 1776 and 1764 cm core depth where *G. puncticulata* occurs in very low percentages (Fig. 3).

In core PS2708-1, SU IV mostly contains Pliocene foraminifers, although a few Paleogene forms are frequent in some intervals, while in core PS2704-1 the foraminiferal assemblages in SU IV are dominated by Paleogene microfaunas. The remaining fraction of the foraminiferal association is characterized by Pliocene species (Fig. 3).

Because the Eltanin core E13-4 was in an incomplete state and strongly fragmented 30 yr after its recovery, the original sediment structure could not be recognized when the core was re-sampled for this study. The sediments below the ejecta horizon (1298 cm core depth) have formerly been interpreted to represent a continuous Eocene section (Wei, 1993). However, discovery of samples consisting of zeolithic clays that are barren in calcareous microfossils indicates that the sediments below the ejecta horizon are disturbed and belong to SU IV (Gersonde et al., 1997). Due to the incomplete state of the core, we could not distinguish whether samples studied herein originates from clasts or the associated matrix. In general the encountered calcareous nannofossil assemblages differ from those obtained in the cores PS2704-1, PS2708-1, and PS2709-1. Com-

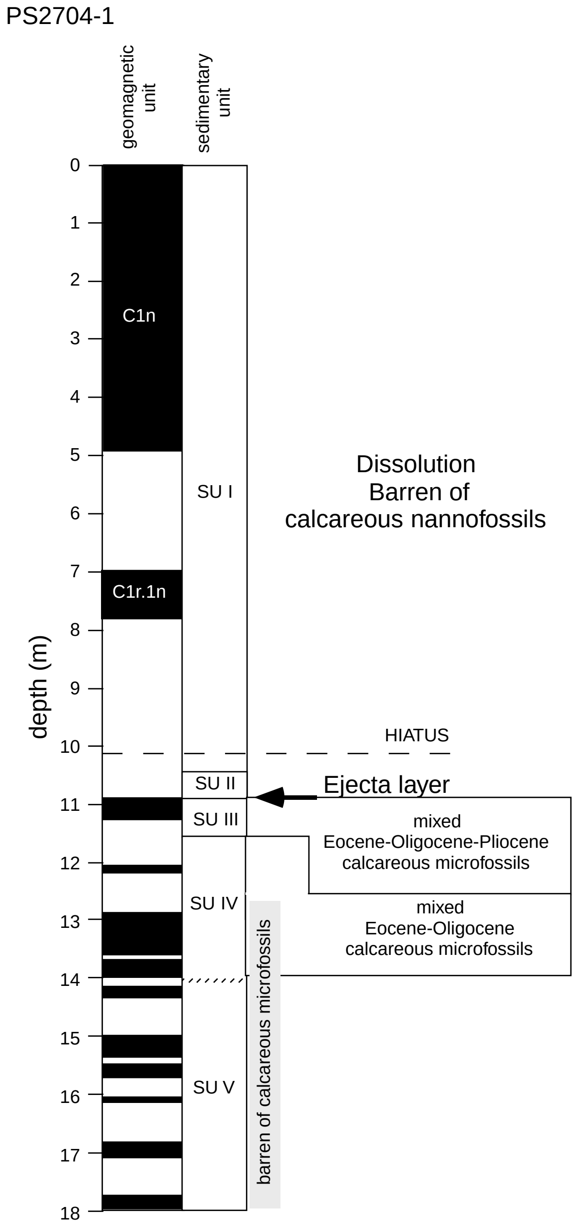

Fig. 4. Occurrence of calcareous microfossils in core PS2404-1. Geomagnetic polarity record and its stratigraphic interpretation as well as assignment of sedimentary units (SU) is according to Gersonde et al. (1997) CN = Calcareous nannofossils. Details of calcareous nannofossil composition given in Table 2.

mon occurrences of *Discoaster sublodoensis*, whose FO is situated at the base of NP14, as well as the presence of *Discoaster lodoensis* (FO at the base of

NP12 and last occurrence (LO) in middle NP14 at about 50 Ma; Perch-Nielsen, 1985; Berggren et al., 1995), allow us to interpret a late early Eocene to early middle Eocene age for most of the samples in this interval. This represents the oldest stratigraphic age obtained from sedimentary sequences that document the impact.

3.2.2. Sedimentary units III and II

The laminated deposits of SU III are interpreted to be sedimented from highly turbulent environments and reflect rapid sedimentation of well-sorted sand-sized particles (Gersonde et al., 1997). The sand fraction of SU III is mainly composed of planktic foraminifers making up to 80% of the bulk sediment. The presence of such sediments in the abyssal basin (PS2704-1) documents that there was an impact-related down slope gravitational sediment transport from the seamount system. Its occurrence on the top of the seamount indicates rapid sedimentation from sediments stirred up in to the water column. Interestingly, we observe a decrease of the amount of Paleogene taxa with decreasing water depth. In the core recovered from the abyssal basin east of the seamounts (PS2704-1), the planktic foraminifers in SU III are dominated by Paleogene taxa, such as *S. angiporoides, G. index, Subbotina linaperta, A. primitiva* and *Catapsidrax dissimilis*. The remaining portion of the planktic foraminifers assemblage is Pliocene in age (Fig. 3). In contrast, in core PS2708-1 taken at the slope of the San Martin Seamounts, Eocene taxa amount to about 30% while the rest are Pliocene taxa. The assemblages obtained from core PS2709-1 recovered at the crest of the seamount are dominated by Pliocene taxa such as *G. puncticulata* and *Neogloboquadrina pachyderma* (sinistral), contributing between 80% and 90% to the total assemblages. The remaining portion is composed of Paleogene species, such as chiloguembelinids and subbotinids. Calcareous nannofossils make up only minor portions in SU III and the species are similar in the three investigated cores. The most characteristic species are *R. umbilica, R. bisecta, Istmolithus recurvus, Discoaster* spp., *Ericsonia formosa* and *Cyclicargolithus floridanus*, all pointing to Eocene and Oligocene ages of the reworked sediments, together with *C. pelagicus* and *C. leptoporus*, both frequent taxa in Neogene sediments.

The sediments assigned to SU II are fine-grained, generally graded and include meteoritic ejecta and reworked sediment. At the base of this unit highest concentration of meteoritic ejecta, the so-called ejecta layer, has been encountered. This sedimentary unit records rapid settling of most probably airborne meteoritic ejecta and deposition from a cloud of resuspended bottom sediment through the water column. Due to the rather rapid settling rate, thick deposits of SU II, as encountered in core PS2708-1, are not disturbed by bioturbation (Gersonde et al., 1997). In the non-bioturbated SU II of core PS2708-1 we found an upward-decrease of Eocene foraminifers from 80% to 20% of the total assemblages. In the abyssal core PS2704-1, no calcareous microfossils were encountered due to carbonate dissolution (Fig. 4). In contrast to SU III, SU II contains high amounts of calcareous nannofossils in the cores recovered above the CCD (PS2708-1, PS2709-1), which document the settling of fine-grained sediment stirred-up in the water column by the impact. The calcareous nannofossil assemblages observed in these cores are the similar to those described from SU III, containing variable proportions of Oligocene and Neogene species such as *Coccolithus miopelagicus*, *Reticulofenestra pseudoumbilicus* and *I. recurvus*. In PS2708-1 around 90% of the calcareous nannofossil assemblages of SU II consist of reworked Paleogene taxa, showing a sharp decrease in the uppermost portion of SU II where the composition of the rapidly accumulated sediments start to be influenced by bioturbation. The assemblages in the following late Pliocene portion of SU I are only affected by minor admixtures of Paleogene taxa (Fig. 2). A different pattern occurs in the SU II section obtained in PS2709-1. Here, the maximum of reworked Paleogene taxa reaches up to 80% of the total assemblages, and in the lowermost portion of SU I up to 20% of the total calcareous nannofossil assemblages can consist of Paleogene species (Fig. 5), together with rare occurrences of Paleogene foraminifers (in particular *C. cubensis*). This pattern can be explained by bioturbation, which affects the rather thin SU II section in PS2709-1

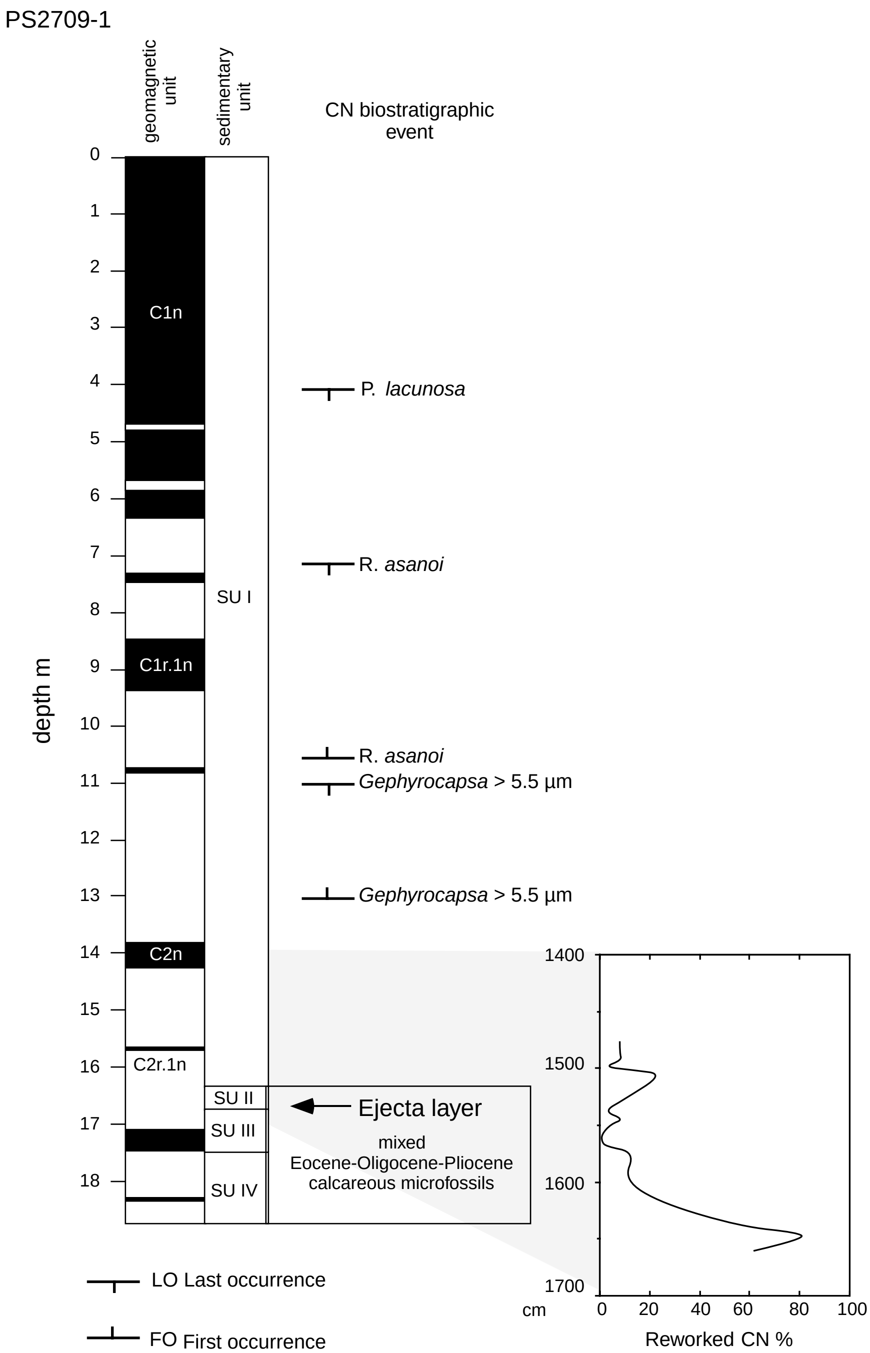

Fig. 5. Calcareous nannofossil biostratigraphic events and correlation with the geomagnetic signal, and relative abundance of reworked calcareous nannofossil and planktic foramnifers in core PS2409-1. Geomagnetic polarity record and its stratigraphic interpretation as well as assignment of sedimentary units (SU) is according to Gersonde et al. (1997). CN = Calcareous nannofossils. Details of calcareous nannofossil composition given in Tables 2 and 3.

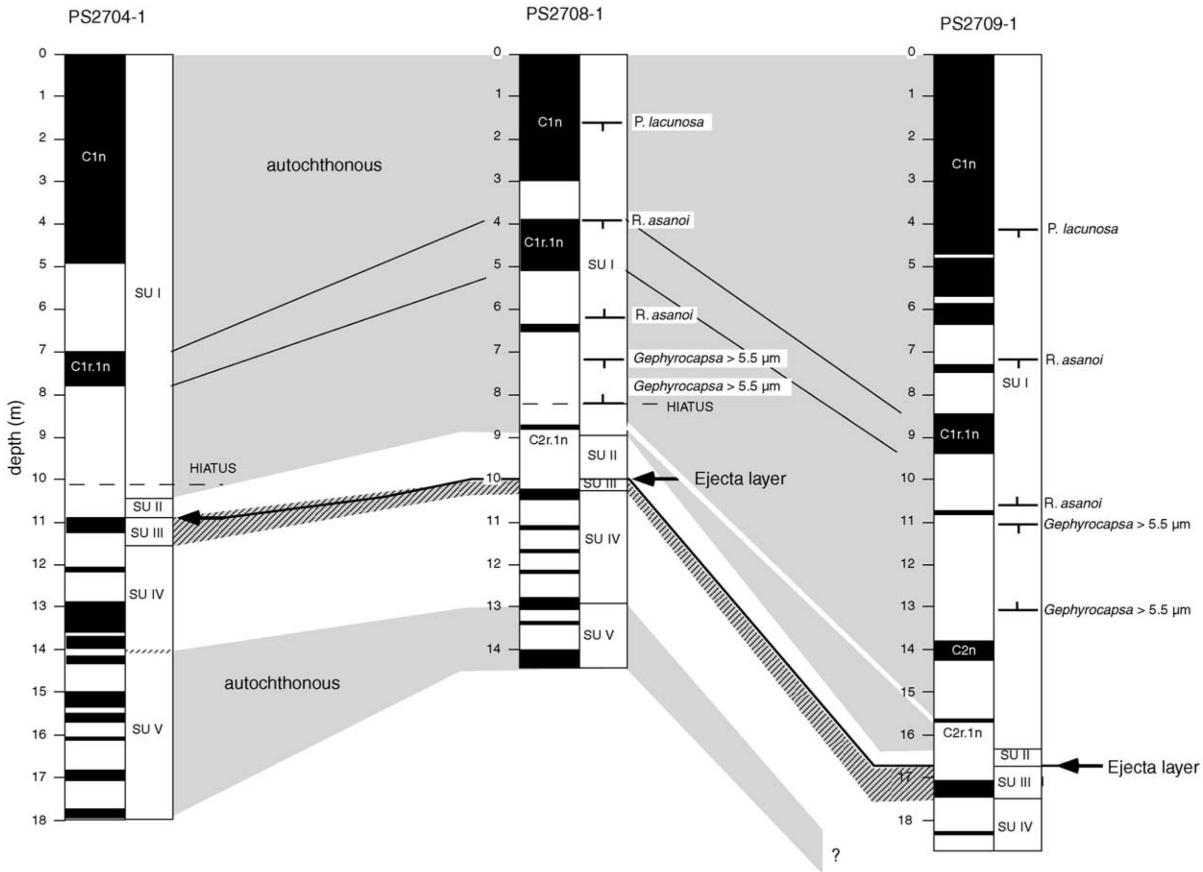

Fig. 6. Correlation of biostratigraphic and paleomagnetic events and sedimentary units of cores PS2709-1, PS2708-1 and PS2704-1.

and leads to an up section admixture of reworked Paleogene taxa.

3.3. Post-impact deposits—sedimentary unit I

This unit (SU I) comprises bioturbated calcareous and biosiliceous sediments deposited after the impact. The degree of preservation of the calcareous nannofossils varies from poor to good in cores PS2709-1 and PS2708-1 (Tables 3 and 4). Core PS2704-1 is devoid of calcareous nannofossils because of its location below the CCD. Here we focus on the dating of the lowermost section of SU I, as an indicative age for the asteroid impact. Comprehensive information on the calcareous nannofossil stratigraphy from the middle and upper portion of SU I in PS2708-1 and PS2709-1 is presented in Flores et al. (2000).

Common records of *Pseudoemiliania lacunosa* and the absence of *R. pseudoumbilicus* which has its LO at ca. 3.8 Ma (Gartner, 1990; Rio et al., 1990; Raffi and Flores, 1995; Flores et al., 1995) indicate a late Pliocene age of the lowermost portion of SU I. Because some other prominent upper Pliocene calcareous nannofossil markers, such as taxa of genus *Discoaster* and *Calcidiscus macintyrei* are absent, a more precise dating of this interval, based on the calcareous nannofossil occurrence pattern, was impossible. The lack of the warmer water taxa *Discoaster* spp. and *C. macintyrei* is interpreted to be related to the presence of a cold-water environment in this region. Gersonde et al. (1997) placed the impact age in the late Pliocene *Thalassiosira kolbei-Fragilariopsis matuyamae* diatom zone and identified the geomagnetic polarity event, which occurs in the lowermost portion of SU I immediately above the impact-related deposits to represent C2r.1n. This event has an age between 2.15 and 2.14 Ma, according to Cande and Kent (1995). The FO of *Gephyrocapsa* $>5.5\,\mu m$, dated at 1.44 to 1.453 Ma (Raffi et al., 1993; Wei, 1993), was observed at 1300 cm in core PS2709-1, allowing the identification of the paleomagnetic reversal recorded at 1400 cm as Chron C2n (Olduvai) (Figs. 4 and 6). In core PS2708-1, the FO of *Gephyrocapsa* $>5.5\,\mu m$ occurs at 825 cm, marked by a disconformity as derived from diatom biostratigraphic results (Gersonde et al., 1997). Due to the presence of this disconformity the period including Chron C2n is absent in this core (Fig. 2). The LO of *Gephyrocapsa* $>5.5\,\mu m$, dated at 1.240–1.227 Ma (Raffi et al., 1993; Wei, 1993) in cores PS2709-1 and PS2708-1 predates a brief geomagnetic episode of normal magnetic polarity, which was interpreted to represent C1r.2r-1n (Cobb Mountain event) (Figs. 2 and 5). According to Wei (1993), the species *Reticulofenestra asanoi* ranges between 1.07 and 0.95 and 0.88 Ma its presence in the above-mentioned cores allows the identification of subchron C1r.1n (Jaramillo).

4. Discussion

4.1. Mixture evaluation and sedimentary reconstruction

Displaced sediments ranging in age from Eocene to Pliocene characterized the impact-related sediment interval, consisting of sedimentary units IV to II. The age and lithologies of clasts deposited in SU IV are similar to those of the sediments identified in SU V (Middle Eocene in PS2708-1) plus others including typical Oligocene and Neogene calcareous planktic microfossils. Samples from SU III in core PS2704-1 contain abundant, well-preserved Paleogene and Pliocene foraminifers (Fig. 3), although this unit was located well below the CCD at the time of the impact. The presence of these foraminifers indicates down-slope transport from the seamount. The preservation of foraminifers in sediments well below the CCD is anomalous and can only be explained by rapid burial during deposition. The finding of a single meteoritic fragment, 1.5 cm in length, in the top portion of SU III in PS2904-1 indicates, that the deposition of SU III at this site did not conclude until 4 h after the impact, considering a settling rate of $37\,cm\,s^{-1}$ of the fragment and the water depth of around 5000 m (Gersonde et al., 1997). Besides the calcareous components documenting gravitational down-slope transport into the abyssal basins, the presence of clasts devoid of calcareous plankton, probably originating from abyssal areas (sub CCD), at intermediate water depths (PS2708-1) indicates impact-related up-slope transport (Gersonde et al., 1997).

Even more complicate is the interpretation of the laminated foraminiferal ooze of SU III recovered on the seamount crest (PS2709-1). These sediments are upward graded as documented by the upward decrease in the fraction $>62\,\mu m$ (below referred as coarse-grained fraction). However, the fragmentation index shows an upward reduction of fragmented foraminiferal shells, a pattern that cannot be explained yet (Fig. 3). Because the re-deposited foraminifers mainly consist of Pliocene taxa, it can be speculated that the foraminifers have been rapidly re-deposited from a stirred up sediment mainly originating in those portions of the seamount system that were located above the CCD. The rather small admixture of Paleogene taxa may be interpreted to indicate that Paleogene deposits from the seamount crest have not been strongly affected by the impact. However, the apparent differences in the grain size distribution of Paleogene and Pliocene sediments recovered in the area of the San Martin Seamounts also may affect the abundance and age distribution of the calcareous microfossils from the impact-related sedimentary units IV-II. The calcareous Paleogene sediments contain a relatively low proportion of coarse-grained particles, which is dominated by well preserved planktic foraminifers, as documented in SU V of core PS2708-1 (Fig. 3). This can be related to the low ratio between foraminifers and calcareous nannofossils in the Paleogene deposits and to the generally small size-range of foraminifers from Paleogene sediments, resulting in a higher proportion of these forms in the finer-grained fractions. Calcareous Pliocene sediments from SU I in cores PS2709-1 and PS2708-1 contain relatively larger amounts of coarse-grained biogenic particles. The effect of different size fractions of the Pliocene and Paleogene foraminifers on the age and abundance pattern of calcareous microfossils is nicely documented by the occurrence of significant amounts of Paleogene foraminifers in the predominantly fine-grained sediments of SU II recovered in PS2708-1, while their occurrence in the more coarser-grained SU III of the same core is less important (Fig. 3). The described pattern indicates that on the seamount Paleogene deposits also were affected and disturbed significantly by the impact event. This is also supported by the overwhelming occurrence of Paleogene calcareous nannofossils in the SU II sediments deposited above the CCD (Figs. 2 and 5). Reasons for the dominant occurrence of Paleogene foraminifers in the SU III sequence of the abyssal core PS2704-1 may be twofold: The relatively small-sized Paleogene foraminifers in this turbidite may be abundant because of sorting effects within the down-slope gravitational flow that did not allow the transport of the generally coarser-grained Pliocene taxa into the depositional area of PS2704-1. Additionally, Paleogene foraminifers in the abyssal core PS 2704-1 also could originate in sediments now at abyssal depths. Considering that basement age in the impact area is Paleocene, according to Cande and Kent (1995), Paleocene foraminifers could have been originally deposited in this area within shallower water depth (above the CCD). Yet no foraminifers-bearing Paleogene sediments are known from the impact area, but recent comprehensive coring around the San Martin Seamounts also may have recovered such sediments (Gersonde, 2002).

4.2. Paleoenvironmental Reconstruction after impact

The sedimentary unit I includes late Pliocene and Pleistocene calcareous nannofossil assemblages (Tables 3 and 4) characteristic of Subantarctic-Antarctic regions (Gard and Crux, 1991; Wei and Wise, 1992; Flores et al., 2000). The abundance and species distribution pattern of these assemblages do not indicate significant changes between the period immediately after the impact (2.15 Ma) and about 1 Ma. However, the relatively low sedimentation rates and extensive bioturbation of the post-impact sediments preclude the documentation of the paleoenvironmental development following immediately after the impact. Only studies based on high-resolution sampling from material deposited at high sedimentation rates may reveal short-term changes related to the impact. Such studies may indicate if there is a close relationship between the impact and distinct climatic changes such as the Marine Isotope Stage 82, a distinctly cold glacial period (Shackleton et al., 1995) that occurs at or close to the time of the impact event.

To date there is no indication for a global environmental response to the Eltanin impact that is recorded by the distribution pattern or the evolution of calcareous nannofossils. In the Atlantic and in the Equatorial Pacific, a distinct reduction of *Discoaster* has been observed at the end of the Pliocene, parallel to a reduction in the total abundance of reticulofenestrid assemblages (Backman and Pestiaux, 1987; Chepstow-Lusty et al., 1992; Flores et al., 1995). This process, however, was progressive during the late Pliocene, and is related to other paleogeographic and climatic changes such as the closure of the Panama Strait and the Northern Hemisphere glaciation (Keigwin, 1978, 1982; Raymo et al., 1989; Shackleton et al, 1984), rather than the impact. A comparable pattern has been observed in analogous situations, such as the Eocene impacts were abrupt changes after the "bombardment" are still unknown (Saunders et al., 1984; Aubry et al., 1990).

Similar to the calcareous nannofossil record, the assemblages of planktic foraminifers do not show any significant changes in the sediment record immediately after the impact. In SU I of core PS2709-1, the late Pliocene assemblage is dominated by *N. pachyderma* (sinistral) together with *Globigerina bulloides* and *G. puncticulata* (ancestor of *Globorotalia inflata*). High co-occurrences of *N.*

pachyderma (sinistral) and *G. bulloides* are indicative for surface water temperatures ranging between about 6°C and 12°C, typical for the area between the Subantarctic Front and the Subtropical Front (Niebler and Gersonde, 1998).

Acknowledgements

The authors thank S. W. Wise, P. R. Bown, K. von Salis and U. Zielinski for their critical and valuable comments. We also acknowledge the revision of the English version of the manuscript accomplished by N.S.D. Skinner and editorial help by A. Deutsch. Research grants CICYT ANT97-1909-E, CLI-1002-CO2-02 and the Spanish-German Integrated Actions supported this study.

References

Aubry, M.P., Gradstein, F.M., Jansa, L.F., 1990. The late early Eocene Montagnais bolide: no impact on biotic diversity. Micropaleontology 36, 164–172.

Backman, J., Pestiaux, P., 1987. Pliocene *Discoaster* abundance variations. Deep Sea Drilling Project Site 606: biochronology and paleoenvironmental implications. Initial Reports of DSDP 94, 903–910.

Berggren, W.A., 1992. Neogene planktic foraminifer magnetostratigraphy of the southern Kerguelen Plateau (Sites 747, 748 and 751). Proceedings of ODP Scientific Results 120, 631–647.

Berggren, W.A., Kent, D.V., Swisher, C.C., Aubry, M.P., 1995. A revised Cenozoic geochronology and chronostratigraphy. In: Berggren, W.A., Kent, D.V., Aubry, M.P., Hardenbol, J. (Eds.), Geochronology Timescales and Global Stratigraphic Correlation. Special Publication 54, Soc. of Economic Paleontologists and Mineralogists, pp. 129–212.

Cande, S.C., Kent, D.V., 1995. Revised calibration of the geomagnetic polarity timescale for the Late Cretaceous and Cenozoic. Geophysical Research 100 (B4), 6093–6095.

Chepstow-Lusty, A., Shackleton, N.J., Backman, J., 1992. Upper Pliocene *Discoaster* abundance from the Atlantic, Pacific, and Indian oceans: the significance of productivity pressure at low latitudes. Memoirs Science Geology 44, 357–373.

Flores, J.A., Sierro, F.J., Raffi, I., 1995. Evolution of the calcareous nannofossil assemblage as a response to the paleoceanographic changes in the Eastern Equatorial Pacific Ocean from 4 to 2 Ma (Leg 138, Sites 849 and 852). Proceedings of ODP, Scientific Results 138, 163–176.

Flores, J.A., Gersonde, R., Sierro, F.J., Niebler, H.S., 2000. Southern Ocean Pleistocene calcareous nannofossil events: calibration with isotope and geomagnetic stratigraphies. Marine Microapleontology 40, 377–402.

Gard, G., Crux, J., 1991. Preliminary results from Hole 704A: Arctic-Antarctic correlation through nannofossil biochronology. Proceedings of ODP, Scientific Results 114, 193–200.

Gartner, S., 1990. Neogene calcareous nannofossil biostratigraphy, Leg 116 (Central Indian Ocean). Proceedings of ODP, Scientific Results 116, 165–187.

Gersonde, R., 2002. The expeditions ANTARKTIS XII/4 (1995) and ANTARKTIS XVIII/5a (2001) of R.V. "Polarstern". Reports on Polar Research, in preparation.

Gersonde, R., Kyte, F.T., Bleil, U., Diekmann, B., Flores, J.A., Gohl, K., Grahl, G., Hagen, R., Kuhn, G., Sierro, F.J., Völker, D., Abelmann, A., Bostwick, J.A., 1997. Geological record and reconstruction of the late Pliocene impact of the Eltanin asteroid in the Southern Ocean. Nature 390, 357–363.

Gersonde, R., Hodell, D.A., Blum, P., 1999. Leg 177 summary: southern ocean paleoceanography. Proceedings of ODP, Initial Reports 177, 1–67.

Keigwin, L.D., 1978. Pliocene closing of the Isthmus of Panama, based on biostratigraphic evidence from nearby Pacific and Caribbean Sea cores. Geology 6, 630–634.

Keigwin, L.D., 1982. Stable isotope stratigraphy and paleoceanography of Sites 502 and 503. Initial Reports of DSDP 68, 445–453.

Keller, G., 1983. Biochronology and paleoclimatic implications of middle Eocene to Oligocene planktic foraminiferal faunas. Marine Micropaleontology 7, 463–486.

Keller, G., 1986. Stepwise mass extinctions and impact events: late eocene to early oligocene. Marine Micropaleontology 10, 267–293.

Keller, G., D'Hondt, S.L., Vallier, T.L., 1983. Multiple microtektite horizons in upper Eocene marine sediments: no evidence for mass extinctions. Science 221, 150–152.

Keller, G., D'Hondt, S.L., Orth, C.J., Gilmore, G.S., Oliver, P.Q., Shoemaker, E.M., Molina, E., 1987. Late Eocene impact microspherules: stratigraphy, age and geochemistry. Meteoritics 22, 25–60.

Kyte, F.T., Brownlee, D.E., 1985. Unmelted meteoritic debris in the Late Pliocene Ir anomaly: evidence for the impact of a nonchondritic asteroid. Geochimica et Cosmochimica Acta 49, 1095–1108.

Kyte, F.T., Smit, J., 1986. Regional variation in spinel compositions: An important key to the cretaceous/tertiary event. Geology 14, 485–487.

Kyte, F.T., Zhou, L., Wasson, J.T., 1981. High noble metal concentration in a late Pliocene sediment. Nature 292, 417–420.

Kyte, F.T, Zhou, L., Wasson, J.T., 1988. New evidence on the size and possible effects of a late Pliocene oceanic impact. Science 241, 63–65.

Margolis, S.V., Claeys, P., Kyte, F.T., 1990. Microtektites, microkristites and spinels from a late Pliocene asteroid impact in the Southern Ocean. Science 251, 1594–1597.

Martini, E., 1971. Standard Tertiary and Quaternary calcareous nannoplankton zonation, In: Farinacci, A. (Ed.), Proceedings of the Second Planktonic Conference Roma (1970). Edizioni Technoscienza, Rome vol. 2, pp. 739–785.
Niebler, H.S., Gersonde, R., 1998. A planktic foraminiferal transfer function for the southern South Atlantic Ocean. Marine Micropaleontology 34, 213–234.
Perch-Nielsen, K., 1985. Cenozoic calcareous Nannofossils. In: Bolli, H.B., Saunders, J.B., Perch-Nielsen, K. (Eds.), Plankton Stratigraphy, Vol. 1. Cambridge University Press, Cambridge, pp. 427–554.
Raffi, I., Flores, J.A., 1995. Pleistocene through Miocene calcareous nannofossils from eastern equatorial Pacific Ocean (Leg 138). Procedings of ODP, Scientific Results 138, 233–286.
Raffi, I., Backman, J., Rio, D., Shackleton, N.J., 1993. Plio-Pleistocene nannofossil biostratigraphy and calibration to oxygen isotope stratigraphies from Deep Sea Drilling Project Site 607 and Ocean Drilling Program Site 677. Paleoceanography 8, 387–408.
Raymo, M.E., Ruddiman, W.F., Backman, J., Clement, B.M., Martinson, D.G., 1989. Late Pliocene variation in Northern Hemisphere ice sheets and North Atlantic deep water circulation. Paleoceanography 4, 413–446.
Rio, D., Raffi, I., Villa, G., 1990. Pliocene-Pleistocene calcareous nannofossil distribution patterns in the Western Mediterranean. Proceedings of ODP, Scientific Results 107, 513–533.
Saunders, J.B., Bernouilli, D., Müller-Merz, E., Oberhänsli, H., Perch-Nielsen, K., Riedel, W.R., Sanfilippo, A., Torrini, R., 1984. Stratigraphy of the late Middle Eocene to Early Oligocene in the Bath Cliff section, Barbados, West Indies. Micropaleontology 30 (4), 390–425.
Shackleton, N.J., Backman, J., Zimmerman, H., Kent, D.V., Hall, M.A., Roberts, D.G., Schnitker, D., Baldauf, J.G., Desprairies, A., Homrighausen, R., Huddlestun, P., Keene, J.B., Kaltenback, A.J., Krumsiek, K.A.O., Morton, A.C., Murray, J.W., Westberg-Smith, J., 1984. Oxygen isotope calibration of the onset of ice-rafting and history of glaciation in the North Atlantic region. Nature 307, 620–623.
Shackleton, N.J., Hall, M.A., Pate, D., 1995. Pliocene stable isotope stratigraphy of Site 846. Proceedings of ODP Scientific Results 138, 337–355.
Sidgurdsson, H., Leckie, R.M., Acton, G.D., et al., 1997. Proceedings of ODP, Initial. Reports, Vol. 165. College Station, TX (Ocean Drilling Program).
Wei, W., 1993. Calibration of upper Pliocene-lower pleistocene nannofossil events with Oxygen Isotope stratigraphy. Paleoceanography 8, 85–99.
Wei, W., 1995. How many impact-generated microspherule layers in the Upper Eocene? Palaeogeography, Palaeoclimatology, Palaeoecology 114, 101–110.
Wei, W., Wise, S.W., 1992. Oligocene-Pleistocene calcareous nannofossils from Southern Ocean Sites 747, 748 and 751. Proceedings of ODP Scientific Results 120, 368–373.